Magnetic domain crossover in FePt thin films

E. Sallica Leva, R. C. Valente, F. Martínez Tabares, and M. Vásquez Mansilla
Centro Atómico Bariloche (CNEA), 8400 Bariloche, Río Negro, Argentina

S. Roshdestwensky
Grupo de Investigación y Servicios a Terceros en el Área de Química, Universidad Tecnológica Nacional, Facultad Regional Resistencia, Chaco, Argentina

A. Butera*
Centro Atómico Bariloche (CNEA) and Instituto Balseiro (U. N. Cuyo), 8400 Bariloche, Río Negro, Argentina
(Received 4 June 2010; revised manuscript received 6 August 2010; published 5 October 2010)

We have investigated the crossover in the magnetic domain structure of FePt thin films as a function of film thickness. We have directly observed by magnetic force microscopy (MFM) that at a critical thickness $d_{cr} \sim 30$ nm the orientation of the magnetization in the magnetic domains changes from in-plane alignment to a system of stripes in which a component perpendicular to the film plane points alternately in opposite directions. The same critical thickness was also estimated from in-plane magnetization vs field measurements. From the MFM images we have also found that the stripe period is an increasing function of the film thickness following a square root law. These data were interpreted with two different models that yield parameters (magnetization, anisotropy, and exchange stiffness) compatible with those determined from magnetization measurements. Films with thicknesses above d_{cr} show a strong dependence of the domain configuration on the magnetic history. Rotatable anisotropy was found in these samples, with a rotational anisotropy field that became stronger with the increase in film thickness. Bubblelike domains could be also observed when the sample is saturated perpendicular to the film plane. All magnetic measurements as a function of film thickness can be interpreted using the same values of magnetization, anisotropy, and exchange stiffness.

DOI: 10.1103/PhysRevB.82.144410 PACS number(s): 75.70.Kw, 75.50.Bb, 75.70.Ak, 75.30.Gw

I. INTRODUCTION

FePt thin-film alloys of equiatomic composition present a great technological interest because of their unique magnetic properties, particularly the very large coercivities and the high-magnetic anisotropy, which can exceed 7×10^7 erg/cm^3 in the ordered fct phase.[1–5] However, as-made films often form in an fcc crystalline-disordered relatively soft magnetic phase,[1,6,7] and the high coercivity, high-anisotropy properties are observed only after proper annealing at elevated temperatures. It was recently reported[6,7] that sputter deposited FePt films in the soft magnetic phase (called A_1) present a critical thickness above which the magnetic domain structure changes from an in-plane planar structure to a periodic stripe array with an out of plane component. A similar stripe structure has been previously observed in several metallic ferromagnetic materials such as Co,[8] FePd,[9,10] Co_3Pt,[11] Permalloy ($Fe_{20}Ni_{80}$).[12,13] This kind of magnetic domain structure is observed in films in which there is a component of the magnetic anisotropy perpendicular to the film plane. The perpendicular anisotropy is in general of magnetocrystalline origin (especially in $L1_0$ alloys) but it could also be due to the combination of stress and a negative magnetostriction coefficient (like in Permalloy films) or surface effects (for example, in multilayers). The transition from planar to stripe domains above a critical thickness, d_{cr}, is due to the minimization of the magnetic energy which can include the contribution of anisotropy, demagnetizing, wall and (if not dealing with the remanent state) Zeeman terms. The critical thickness depends on the material properties such as the anisotropy, the saturation magnetization and the exchange constant. There are several models for the calculation of d_{cr}, see, for example, Refs. 12, 14, and 15, that predict larger values of d_{cr} in materials with a large magnetization, a large exchange, or a small anisotropy. The value of the critical thickness is in the range of 20–30 nm for Co,[8] partially ordered FePd,[16] or disordered FePt films,[6,7] and can take larger values (on the order of 200 nm) in films with lower anisotropy.[13] The ratio between the perpendicular anisotropy energy and the demagnetizing term defines the quality factor, $Q = K_\perp / 2\pi M_s^2$. For $Q > 1$ the magnetization in each stripe is essentially perpendicular to the film surface while for $Q < 1$ the magnetization tends to be in the film plane with an alternating net perpendicular component.[14] FePt films in the A_1 phase can be grown with a [111] texture which induces an out of plane anisotropy of magnetocrystalline origin.[7] Due to the relatively low value of the anisotropy of the soft phase, the effective Q factor in this system is expected to be below one, which allows the study of the thickness dependence of the magnetic properties with different experimental techniques close to d_{cr}. In this work we report the growth and structural characterization of disordered FePt films and focused our attention on the evolution of the magnetic domain structure with film thickness from a planar to a stripe structure.

II. EXPERIMENTAL DETAILS

We have investigated a series of as-made disordered FePt films which have been fabricated by dc magnetron sputtering on naturally oxidized Si (100) substrates. The samples were deposited from an FePt alloy target with a nominal atomic composition of 50/50. The chamber was pumped down to a

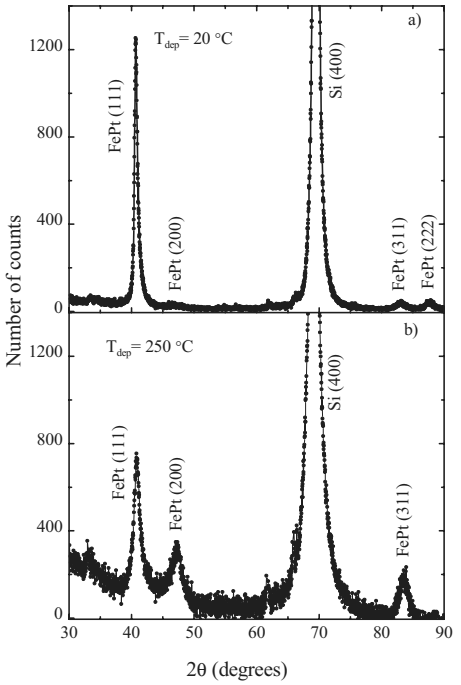

FIG. 1. (a) X-ray diffraction pattern of an FePt film of 94 nm deposited at room temperature. (b) Same as above but deposited at 250 °C.

base pressure of 10^{-7} Torr and the films were sputtered using 2 mTorr of Ar pressure, a power of 20 W and a target-substrate distance of 5 cm. With these parameters we obtained a sputtering rate of 0.15 nm/s. This rate was calculated from a control sample with a mask in which the height step was measured using an atomic force microscope. Eight different films were sputtered in a first batch of samples with thicknesses of: 9, 19, 28, 35, 42, 49, 56, and 94 nm. We have also prepared relatively thick samples (~100 nm) for x-ray diffraction and energy-dispersive x-ray spectroscopy (EDX) studies, and a 30 nm film deposited on a 400 mesh carbon-coated transmission electron microscope (TEM) Cu grid to study the grain size and the microstructure. From the EDX analysis we have found that the Fe/Pt atomic ratio of both the target and the films was approximately 45/55. The magnetization data were measured using a LakeShore model 7300 VSM and the images of the magnetic domains were obtained with a Veeco Dimension 3100 atomic AFM/MFM with Nanoscope IV electronics in which we have adapted a home made electromagnet that can reach a maximum field of ±300 Oe. Magnetic images have been acquired using medium moment, medium coercivity tips from Veeco (MESP) and APPNano (MAGT).

III. EXPERIMENTAL RESULTS AND DISCUSSION

A. X-ray diffraction and microstructure

In [Fig. 1(a)] we show the x-ray diffraction (XRD) pattern of a film of 94 nm deposited at room temperature. All FePt peaks could be indexed as corresponding to the disordered A_1 fcc phase. Apart from the Si reflection arising from the substrate, no other peaks were observed indicating that as-made films grow in the disordered A_1 crystalline phase. From the different reflections we estimated the lattice parameter of the cubic lattice $a=0.3866(2)$ nm. Note that the intensity of the peak corresponding to a plane (111) is much larger than the rest of the diffractions, suggesting a [111] texture perpendicular to the film plane. In particular, the experimental intensity percent ratios $I[200]/I[111]=9$ and $I[311]/I[111]=7$, are considerable smaller than the calculated values for randomly oriented grains: $I[200]/I[111]=45$ and $I[311]/I[111]=22$. The ratio $I[222]/I[111]=8$ is similar to the expected value, within the experimental error. The same kind of texture was reported by Spada *et al.*[17] in FePt films grown on Si wafers with a MgO buffer layer. It is worth mentioning that the [111] direction is an easy cubic magnetocrystalline axis for fcc CoPt with an anisotropy value[18] of $K_{mc}\sim 6\times 10^5$ erg/cm^3 and a similar value is expected in the case of FePt which has the same crystalline structure. In Ref. 17 it is also mentioned that a thermal annealing at temperatures below 250 °C is still low enough to avoid the transformation to the ordered $L1_0$ phase but can relax the tensile strain that is usually observed in as-deposited films. We have then deposited a sample at 250 °C in order to compare the lattice parameter of both films. For the sample fabricated at 250 °C we have obtained $a=0.3840(2)$ nm which is ~0.7% smaller than the lattice parameter of the as-made film, that is $(a_{RT}-a_{250})/a_{RT}=\varepsilon_z=0.0067$. This change is larger than that reported in Ref. 17 (approximately 0.3%), the difference possibly arising from the fact that we have heated the substrate during deposition and the film in Ref. 17 was post annealed. We have also observed [Fig. 1(b)] that when the films are deposited above room temperature the [111] texture is considerably reduced but superstructure peaks are still not detected. As shown in Fig. 2 the lattice parameter of our samples follows the behavior reported in Refs. 18 and 19. Small discrepancies in the lattice parameters are probably due to different preparation methods, the influence of a buffer layer, or the error in the determination of the Fe concentration. Using the Scherrer formula ($D=K\lambda_{K\alpha}/\beta\cos\theta$) that relates the average particle

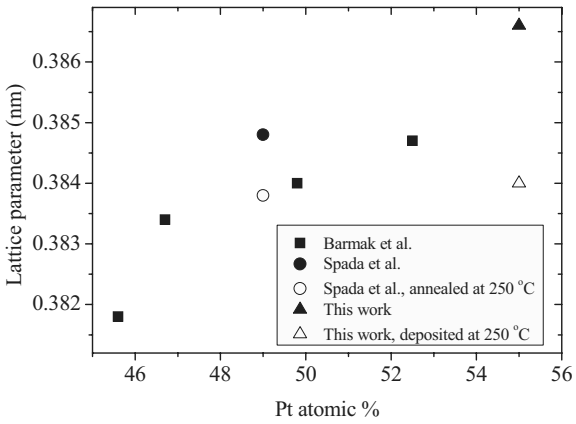

FIG. 2. Lattice parameter of FePt films in the cubic A1 phase. Full symbols correspond to samples deposited at room temperature and open symbols at higher temperatures. Data for comparison have been taken from Ref. 19 (squares) and Ref. 17 (circles).

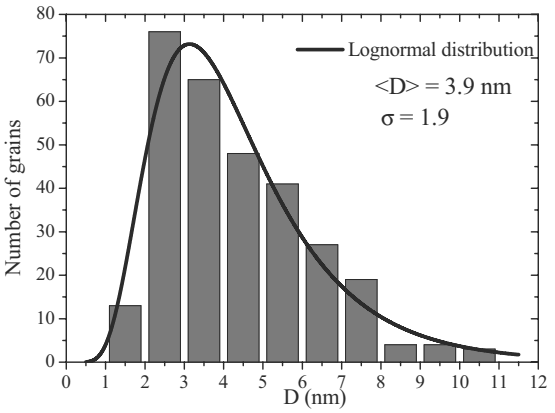

FIG. 3. Grain-size distribution obtained from TEM micrographs. The histogram was fitted with a lognormal distribution.

size D with the diffraction linewidth β, the radiation wavelength $\lambda_{K\alpha}$, and the diffraction angle θ (K is a constant close to 1 for spherical particles), we have made a rough estimation of the grain size using the high angle (311) and (222) reflections. As we shall see when we analyze the particle size through TEM images, the average particle size $D \sim 7.5(7)$ nm obtained from XRD is probably overestimated because of the higher intensity coming from the larger particles. Assuming that after the thermal annealing the lattice is fully relaxed, we can estimate the magnetoelastic anisotropy induced by the in-plane planar compression. We have used the values $\nu=0.33$ for the Poisson's ratio,[17,20,21] and $E=180$ GPa for the Young's modulus.[20,21] The saturation magnetostriction constant of FePt disordered films was reported by Aboaf *et al.*[22] ($\lambda=70\times10^{-6}$), and more recently by Spada *et al.*[17] ($\lambda=34\times10^{-6}$). There are also reported values in FePd films by Shima *et al.*[23] ($\lambda=65\times10^{-6}$) and Wunderlich *et al.*[24] ($\lambda=250\times10^{-6}$, in films prepared at 423 K). Note that in all cases the reported magnetostriction is positive. For our estimation we use a value of $\lambda=70\times10^{-6}$. Assuming an isotropic sample the magnetoelastic anisotropy constant is given by $|K_{me}|=\frac{3}{2}\lambda\sigma_x=\frac{3}{2}\lambda E\nu\varepsilon_z\sim4.2\times10^5$ erg/cm^3. As the stress is compressive and $\lambda>0$ the anisotropy constant is negative, which favors an easy axis perpendicular to the film plane, similar to the effects of the [111] crystalline texture. The magnitude of this anisotropy constant due to magnetoelastic effects is of the same order than K_{mc}.

The 30 nm film deposited on a carbon coated grid was studied by TEM. We have also observed a [111] texture in this sample and measured the size of approximately 500 grains to obtain the size distribution shown in Fig. 3. The lognormal distribution has a mean value $D=3.9$ nm with a standard deviation $\sigma=1.9$. Note that this value is considerable smaller than the average grain size estimated from the linewidth of the XRD peaks. In order to compare the mean value of the grain-size distribution obtained from the TEM micrographs with the estimation made using the Scherrer formula, it should be considered that in XRD experiments the diffracting intensity is proportional to the volume of the grains. One option to compare both values is to weight the TEM size distribution by its corresponding volume. The volume weighted TEM average grain size is then $\langle D\rangle=7.1$ nm ($\sigma=3.5$) which is similar to the XRD estimation. This coincidence is a good indication that the microstructure of films deposited on Si with an amorphous oxide layer is quite similar to that of films deposited on amorphous carbon and also that the grain size does not change significantly with film thickness.

B. Magnetic force microscopy and magnetization measurements

The surface magnetic domain structure of films as-deposited on Si substrates was studied by magnetic force microscopy (MFM). As the tip was magnetized along its axis, the force gradient normal to the film plane is detected in all cases. We have used the tapping lift mode with a second scan separation of 10 nm and phase detection. The small lift distance was necessary due to the relatively weak magnetic signal, especially in thinner films. Scans with larger lift distances were made in order to check that the domain configuration does not change when the lift height is reduced to 10 nm, indicating that the domain structure is not significantly disturbed by the tip stray field. In same cases it was necessary to use a smaller driving amplitude voltage in the second pass in order to avoid the interaction of the tip with the surface.

In general films with thicknesses below 28 nm show the presence of a very limited number of magnetic domains (see Fig. 4). Domain walls are only observable close to the edges of the samples were closure domains are formed. The corresponding in-plane hysteresis loop has a relative large squareness and remanence, which is a strong indication that the magnetization in these samples stays essentially in the film plane. As shown in Fig. 5, films thinner than d_{cr} present a normalized value of the remanent magnetization close to one and a relatively low coercive field. These films also have a very narrow distribution of switching fields (less than 1 Oe in the case of the film of 9 nm) which makes difficult to obtain a well-demagnetized state by standard methods.

The behavior of films with a thickness $d\geq35$ nm is totally different. In this case a periodic stripe structure is observed (right panel of Fig. 4) which indicates that the magnetization has an oscillating component perpendicular to the film plane. The corresponding hysteresis loop is totally consistent with this interpretation. As we will later discuss, the almost linear variation in M between $H=0$ and the in-plane saturation field is related to the alignment of the out of plane component of M with the external field. In films thicker than d_{cr} the remanent magnetization tends to decrease (Fig. 5) suggesting that the out of plane component becomes larger, and the coercive field is always much larger that the values found for $d<d_{cr}$, due to the changes occurring in the domain structure. We show in Fig. 6 another domain pattern obtained in the remanent state for the 94 nm film, after the sample was brought to saturation outside the microscope with a field of 1 kOe. It is observed that the stripe structure is essentially parallel to the direction of the applied field but there are oscillations in the in-plane perpendicular direction that can be quantified by the azimuthal angle ϕ_0. To analyze the distribution in the direction of the stripes from perfect parallel

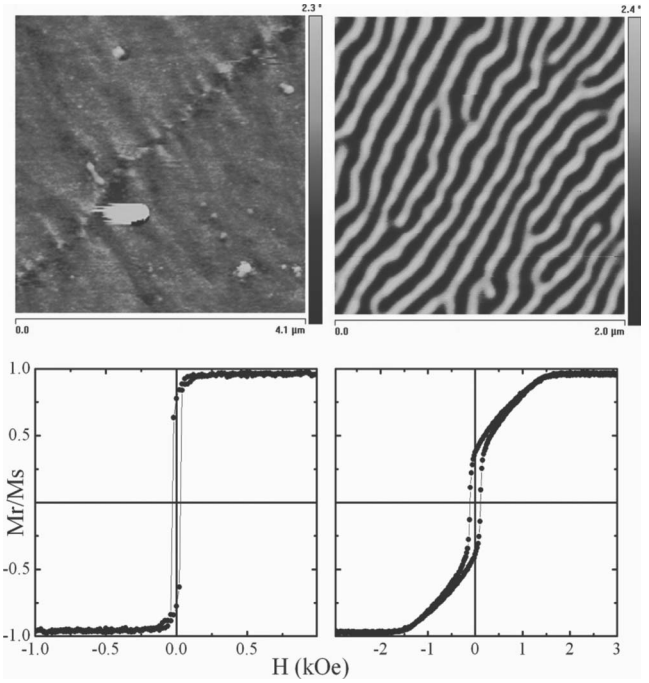

FIG. 4. MFM image of two films with a thickness of 28 nm (left) and 94 nm (right). The x scale is indicated in the figure and is similar to the y scale. The color coded vertical bar represents de phase shift of the cantilever resonance. The domain wall in the thinner film was observed close to the film edge. In both cases the domain structure corresponds to the remanent state obtained after saturating the sample with a magnetic field of 1 kOe applied outside the microscope. The corresponding in-plane hysteresis loops in the bottom panel show the change in the magnetic behavior of the films according to their thickness.

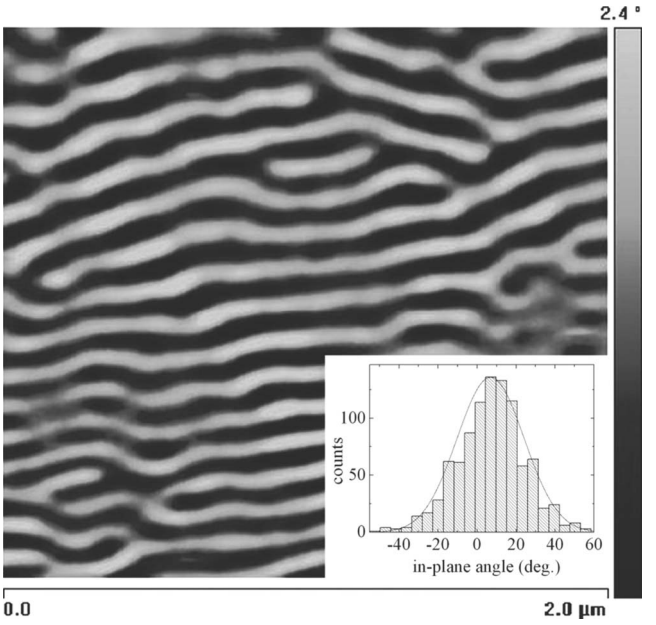

FIG. 6. MFM image of a film with a thickness of 94 nm. The domains correspond to the remanent state obtained after saturating the sample with a magnetic field of 1 kOe applied close to the horizontal direction. The stripe period is approximately 145 nm. In the inset we show the angular distribution of the stripe direction, which can be fitted with a Gaussian function.

alignment we have superposed a grid of 40×40 squares over the image and determined the direction of the stripe edges in each square. We obtained a Gaussian histogram (shown in the inset of Fig. 6) with an average angle of $\phi_0 = 5.6°$ measured from the horizontal direction (this angle is not zero because the sample was saturated outside the microscope and a small misalignment is unavoidable) and a dispersion $\Delta\phi_0 = 16.1°$. We repeated the same procedure in another region of the sample (in this case after saturating with 10 kOe) and obtained a slightly larger value of $\Delta\phi_0 = 17.1°$. The rest of the samples which are thicker than the critical thickness d_{cr} present a similar domain structure but the stripe period depends on the film thickness. The stripe period for the 94 nm film shown in Fig. 6 is $\lambda_s \sim 145$ nm. In Fig. 7 we show the dependence of the stripe half period at remanence as a function of film thickness, obtained from the MFM images. For completeness we have added a few extra points from a sec-

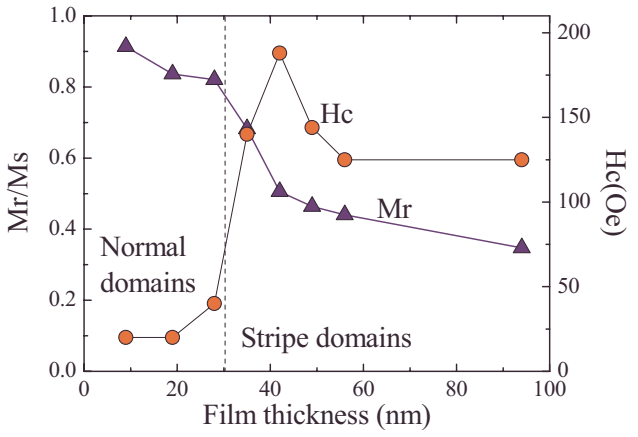

FIG. 5. (Color online) Magnetization remanence and coercive field as a function of film thickness. We have indicated with a vertical line the critical thickness that separates the two magnetic domain regimes.

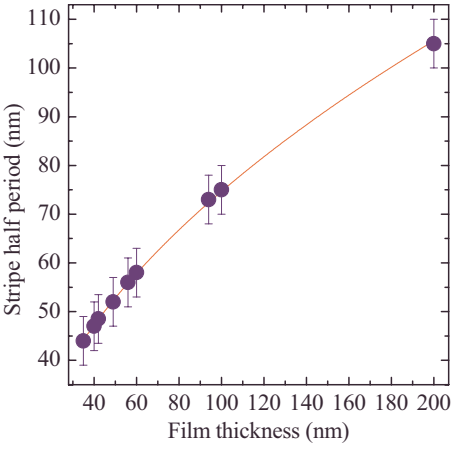

FIG. 7. (Color online) Half period of the stripe structure obtained from MFM images at the remanent state as a function of the film thickness (full circles). We have fitted the observed behavior with a square-root law (continuous line).

ond batch of samples which include a film with a thickness of 200 nm. The stripe period dependence on film thickness was analytically solved by Murayama[25] who proposed the following asymptotic expression in the case of $Q \to 0$,

$$\frac{\lambda_s}{2} \simeq \left[\pi^2 A \left(\frac{1}{2\pi M_s^2} + \frac{1}{K_\perp} \right) \right]^{1/4} \sqrt{d} = \alpha_0^M \sqrt{d}, \qquad (1)$$

where A is the exchange stiffness constant, M_s the saturation magnetization, and $K_\perp$ the perpendicular anisotropy. From M vs H in-plane and out-of-plane loops we have found that both the saturation magnetization and the perpendicular anisotropy are similar for all film thicknesses, and we have assumed the same values for all samples with an average $\langle M_s \rangle = 866(25)$ emu/cm^3 and $\langle K_\perp \rangle = 1.5(4) \times 10^6$ erg/cm^3. In Ref. 1 the value of the stiffness constant is reported to be relatively independent of the degree of chemical order, with an average value $A \sim 0.95 \times 10^{-6}$ erg/cm. To estimate the value of A for our samples that have a 45/55 FePt composition, we measured a magnetization vs temperature curve in a film of 94 nm and found a value of $T_C \sim 500$ K, considerably smaller than the Curie temperature of the equiatomic alloy, $T_C \sim 750$ K. This difference lowers the value of the exchange constant to $A \sim 0.6 \times 10^{-6}$ erg/cm. With these parameters it is possible to estimate the constant factor in Eq. (1), $\alpha_0^M = 4.7(5)$ nm$^{1/2}$. The experimental data can be very well fitted with a square root dependence of the stripe period with the film thickness. Note that this result is supporting the assumption that the whole set of films may be described with the same values of A, M_s, and $K_\perp$. The best fit, that is also shown in Fig. 7, gave a value of $\alpha_0 = 7.4(2)$ nm$^{1/2}$, which is somewhat larger than that estimated from Eq. (1). This difference suggests that the films may have a larger exchange stiffness constant and/or a lower M_s or $K_\perp$. However, due to the 1/4 power dependence of α_0^M, considerably large departures of the parameters from their estimated values are necessary to explain the differences between model and experiment. As already mentioned the applicability of Eq. (1) is expected to hold only in the case very small Q. Our films have a $Q = 0.32(8)$, so that discrepancies between experiment and theory may arise due to the limited validity of Eq. (1). In the paper of Murayama[25] the same discrepancy was observed in films with $Q \sim 0.17$. The dependence of the stripe period with the film thickness in the case $Q \geq 1$ has been treated by Kooy and Enz.[26] In Ref. 8 the authors give an analytical expression which was applied to explain the stripe structure of Co films with $Q \sim 0.4$,

$$\frac{\lambda_s}{2} \simeq \left[\frac{\pi^2 \sqrt{A K_\perp}}{8 M_s^2} \left(1 + \sqrt{1 + \frac{2\pi M_s^2}{K_\perp}} \right) \right]^{1/2} \sqrt{d} = \alpha_0^K \sqrt{d}. \quad (2)$$

In this case the estimation of the coefficient $\alpha_0^K = 6.9(4)$ nm$^{1/2}$ is much closer to the experimental value $\alpha_0 = 7.4$ nm$^{1/2}$. Although a full micromagnetic simulation would be needed to obtain a better description of the stripe period as a function of the film thickness, the two simple models discussed above are consistent with the choice of parameters $(A, M_s, K_\perp)$ and give a very reasonable estimation for the description of the experimental measurements.

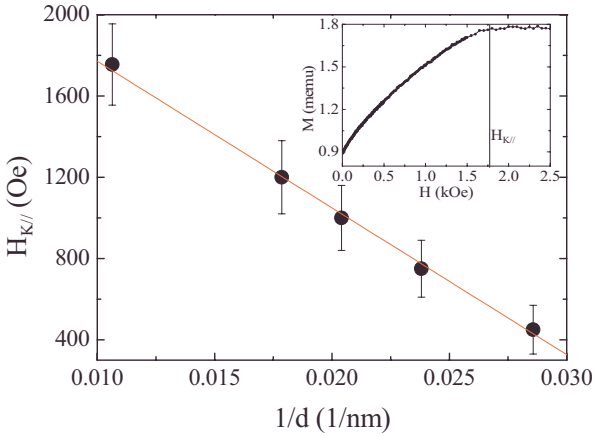

FIG. 8. (Color online) In-plane saturation field as a function of the inverse of the film thickness (solid circles). The curve was fitted with a linear law (continuous line). In the inset we show one quadrant of a M vs H loop for the film of 94 nm where we have indicated the saturation field.

Another experimental test that can be done to check the invariance of the parameters M_s, and $K_\perp$ with film thickness is to measure the necessary in-plane field $(H_{K\|})$ to align the magnetization with the applied field. According to Murayama[25] this field is related with the film thickness through the formula,

$$H_{K\|} \sim \frac{2K_\perp}{M_s} - \frac{2K_\perp}{M_s} \frac{1}{\sqrt{1 + K_\perp / 2\pi M_s^2}} \frac{d_{cr}}{d}. \qquad (3)$$

In Fig. 8 we show the experimental data of $H_{K\|}$ as a function of $1/d$, together with a linear fit. It can be seen that the experimental points follow very well a linear law, from which we can extract (assuming M_s as a known parameter) the values of d_{cr} and $K_\perp$. We have obtained $d_{cr} = 32(6)$ nm and $K_\perp = 1.1(2) \times 10^6$ erg/cm^3 which are totally consistent with the values obtained from the MFM images. The estimation of the critical thickness in zero field for very low Q materials[14] is given by $d_{cr} \sim 2\pi\sqrt{A/K_\perp} = 39(6)$ nm. In our films with $Q = 0.32$ the critical thickness is reduced approximately by 70% (see Fig. 3.109 of Ref. 14) giving $d_{cr} = 28(4)$ nm which is within the experimental error of the critical thickness estimated by MFM.

Another interesting behavior that we have observed for films thicker than the critical thickness is the strong dependence of the domain configuration at remanence on the magnetic history. In Fig. 9 we show the MFM images of the same film that was subjected to different field sequences. In the top panel it is observed that an almost parallel stripe structure is always formed in the direction where a strong in-plane field is applied. If a field of strong enough magnitude is applied in another direction the whole structure rotates rigidly to the new direction. This effect, known as rotatable anisotropy, was reported a long time ago by several authors,[27–29] and was explained to arise from magnetostriction and residual stress effects due to the external applied field that creates an easy axis along the direction of the saturating field. The remanent state was also studied in the case of demagnetized

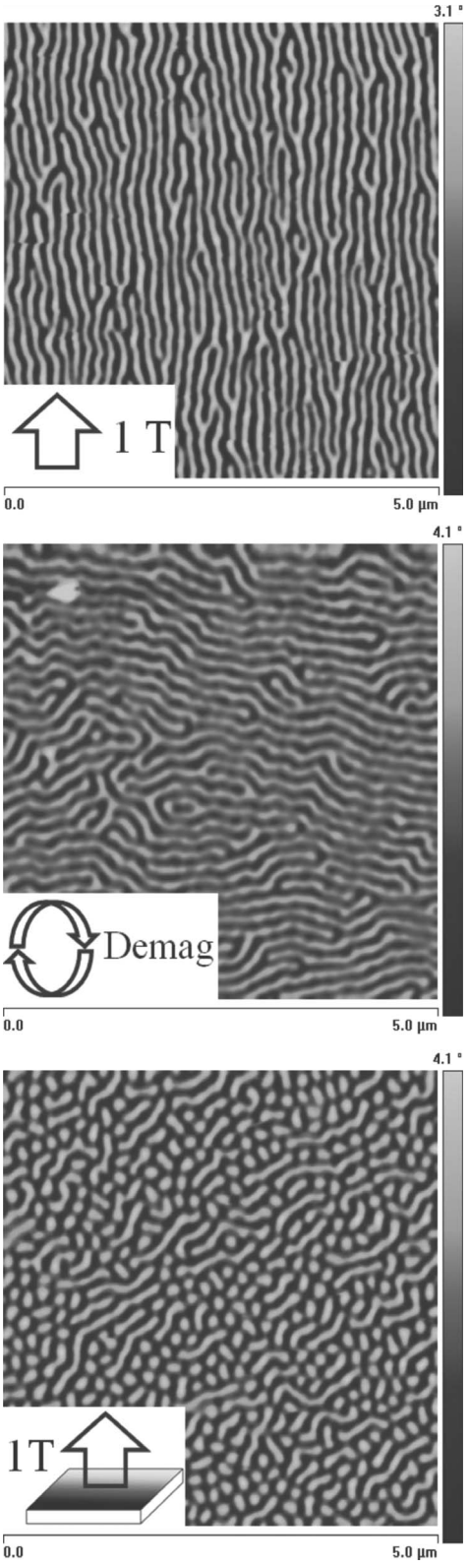

FIG. 9. Magnetic domain structure at remanence in a film of 94 nm for different cases. Top image corresponds to a measurement made after saturating the sample in the vertical direction with an in-plane field of 10 kOe (1 T). The central image was obtained after demagnetizing the film in an in-plane rotating field of decreasing amplitude. In the bottom image the saturating field of 10 kOe was applied perpendicular to the film plane.

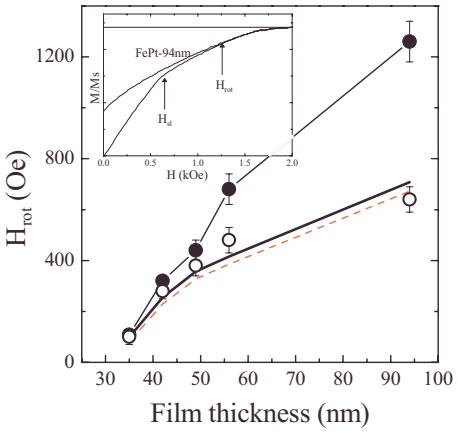

FIG. 10. (Color online) Minimum transverse field necessary to rotate the stripe structure by 90° (H_{rot}, full circles) and field where a change in slope is observed (H_{sl}, open circles) as a function of film thickness. As shown in the inset of the figure, H_{rot} and H_{sl} are defined as the fields above which a reversible behavior and a change in slope are observed in the M vs H curves, respectively. The continuous and dashed lines have been obtained from Eq. (4) assuming $\Delta\phi=0°$ and $\Delta\phi=16°$, respectively.

films and samples saturated with a field applied perpendicular to the film plane. If the sample is demagnetized with a sequence of decreasing fields applied in a fixed direction the MFM pattern is quite similar to the top panel of Fig. 9. Another method often used to demagnetize films consists in rapidly rotating the sample in an in-plane field of decreasing amplitude (Fig. 9 central panel). In this case the stripes tend to form in a more labyrinthic pattern, as expected for a demagnetizing field that changed its direction while it was decreased. The bottom panel of Fig. 9 corresponds to the remanence domain pattern obtained after the sample was saturated with a perpendicular field of 10 kOe. In this situation the domain structure is a mixture of bubbles and short stripes. In the case of a film saturated in the out-of-plane direction the formation of metastable bubble domains can occur when $Q > 1$, which is suggesting that in this configuration the external field is contributing to enhance the perpendicular anisotropy. The apparent alignment of the stripes in the same direction is probable due to a small sample misalignment when applying the perpendicular saturating field.

When the transverse saturation field is not strong enough to fully rotate the stripe structure, the remanent state consists of almost parallel stripes that form an angle with the direction of the applied field. The minimum field needed to rotate the stripe structure by 90° was estimated with VSM measurements using the following sequence:[30] the sample was first saturated with a field of 10 kOe in an arbitrary in-plane direction and rotated in the film plane by 90° in zero field, the magnetization was then measured increasing and decreasing the magnetic field. We define the rotational field (H_{rot}) as the field above which the curve becomes reversible. In order to check that the stripe structure was fully rotated for fields larger H_{rot} we measured with MFM the domain structure of the remanent state after the application of a transverse saturation field below and above H_{rot}. In Fig. 10 we show the dependence of H_{rot} with film thickness where it can be ob-

served that this field increases considerably in the thicker films. A similar dependence with film thickness was observed Lehrer *et al.*[29] in Ni films. The origin of this dependence is still not clear. If the rotatable anisotropy was due to magnetostrictive effects only, the maximum induced anisotropy field that we could expect is on the order of $2K_{ind}/M_s \sim 3\lambda^2 E/M_s \sim 30$ Oe and independent of film thickness. A model for the film thickness dependence of the rotatable field in a system of parallel stripes was discussed in Ref. 31. In that paper it was argued that the presence of a small transverse effective field can cause a pseudouniaxial anisotropy with the easy axis aligned in the direction of the stripes. The value of this anisotropy field is given by,

$$H_K \sim 8M_s \frac{J_2^2(\theta_0)}{J_0(\theta_0)}\left[\pi - \frac{\lambda_s}{2d}(1 - e^{-2\pi t/\lambda_s})\right] \sim 8M_s \frac{J_2^2(\theta_0)}{J_0(\theta_0)}\left(\pi - \frac{\lambda_s}{2d}\right), \quad (4)$$

where J_n are Bessel functions of the first kind and θ_0 is the out of plane equilibrium angle for the magnetization at zero applied field, measured from the film plane. This angle can be obtained from the M_r/M_s ratio ($M_r/M_s = \cos\theta_0 \cos\phi_0$) of the hysteresis loops assuming that $\cos\phi_0 = 1$, i.e., M has no in-plane component perpendicular to the stripe axis. The values of H_K are also plotted in Fig. 10 for comparison with H_{rot}. It can be seen that there is a good coincidence for the lower values of d while some discrepancies are found for $d \geq 56$ nm. A deviation of the magnetization vector from the direction parallel to the stripe axis (see Figs. 6 and 9) would give a smaller value of H_K but with the values of $\Delta\phi_0 \sim 16°$ estimated from the MFM images no significant corrections are expected, as can be seen by the dashed curve in Fig. 10. When analyzing the experimental data it must be kept in mind that H_{rot} is an upper limit for the anisotropy because it is determined as the field where the domain structure rotates completely. H_K, on the other hand, is an average value for this anisotropy and hence is expected to be lower than H_{rot}. In the inset of Fig. 10 it can be seen that there is a change in the slope of the magnetization at a field of $H_{sl} \sim 650$ Oe. See that this change is not present in the returning branch of the loop and one could be tempted to assign it to the irreversible rotation of the in-plane anisotropy. The field H_{sl} has been also plotted in Fig. 10 where it can be seen that it follows closely the theoretical model. H_{sl} is considerable lower than H_{rot} for the thicker films but has almost the same value in thinner samples in which the slope change is coincident with the irreversibility. Unfortunately our MFM system is presently limited to a maximum in-plane field of 300 Oe so that we are not able to directly observe the rotatable behavior. We also like to stress that the model of Ref. 31 has been developed for the case of parallel stripes of equal period with a sinusoidal magnetization profile. These requirements are not completely fulfilled in all our films so that some discrepancies between the model and the experimental data can be expected.

IV. CONCLUSIONS

We have studied the structural and magnetic properties of FePt alloy films as a function of film thickness. We have found that above a critical thickness the magnetic domain structure evolves to a system of almost parallel stripes due to the presence of a perpendicular anisotropy. This anisotropy is originated by the crystalline [111] texture and also by magnetostrictive effects. The dependence of the stripe period, the in-plane saturation field and the rotatable anisotropy with d has been explained with different models. All results indicate that the magnetic behavior for different film thicknesses can be correctly described with the same values of magnetization, anisotropy and exchange stiffness. Additional studies and modeling are needed to explain the formation of metastable domain structures when the saturating field is applied perpendicular to the film plane or in the case of a circular demagnetizing field. Micromagnetic simulations using the OOMF package are presently under way in order to better understand the magnetic behavior in these situations. In the magnetization measurements of thicker films, where rotatable anisotropy is observed, it is difficult to separate the irreversible in-plane rotation from the alignment of the out of plane component of M. We are presently trying to adapt our MFM system in order to obtain images of the magnetic domains not only at remanence but also at fields close to H_{rot}.

ACKNOWLEDGMENTS

This was supported in part by Conicet under Grant No. PIP 112-200801-00245, ANPCyT under Grant No. PME # 1070, and U.N. Cuyo under Grant No. 06/C235, all from Argentina. We would like to acknowledge very fruitful discussions with Carlos A. Ramos and Emilio de Biasi. Technical support from Julio C. Pérez and Rubén E. Benavides is also acknowledged.

*Also at Consejo Nacional de Investigaciones Científicas y Técnicas; butera@cab.cnea.gov.ar

[1] S. Okamoto, N. Kikuchi, O. Kitakami, T. Miyazaki, Y. Shimada, and K. Fukamichi, Phys. Rev. B **66**, 024413 (2002).

[2] K. R. Coffey, M. A. Parker, and J. K. Howard, IEEE Trans. Magn. **31**, 2737 (1995).

[3] R. A. Ristau, K. Barmak, L. H. Lewis, K. R. Coffey, and J. K. Howard, J. Appl. Phys. **86**, 4527 (1999).

[4] S. Jeong, Y.-H. Hsu, D. E. Laughlin, and M. E. McHenry, IEEE Trans. Magn. **37**, 1299 (2001).

[5] R. F. C. Farrow, D. Weller, R. F. Marks, M. F. Toney, S. Hom, G. R. Harp, and A. Cebollada, Appl. Phys. Lett. **69**, 1166 (1996).

[6] M. Vásquez Mansilla, J. Gómez, and A. Butera, IEEE Trans. Magn. **44**, 2883 (2008).

[7] M. Vásquez Mansilla, J. Gómez, E. Sallica Leva, F. Castillo Gamarra, A. Asenjo Barahona, and A. Butera, J. Magn. Magn.

Mater. **321**, 2941 (2009).
[8] M. Hehn, S. Padovani, K. Ounadjela, and J. P. Bucher, Phys. Rev. B **54**, 3428 (1996).
[9] V. Gehanno, Y. Samson, A. Marty, B. Gilles, and A. Chamberod, J. Magn. Magn. Mater. **172**, 26 (1997).
[10] A. Asenjo, J. M. García, D. García, A. Hernando, M. Vázquez, P. A. Caro, D. Ravelosona, A. Cebollada, and A. Briones, J. Magn. Magn. Mater. **196-197**, 23 (1999).
[11] L. Folks, U. Ebels, R. Sooryakumar, R. Rokhlin, D. Weller, and R. F. C. Farrow, Proc. Magneto-Optical Recording Int. Symp. **23**, 85 (1999).
[12] R. Bručas, H. Hafermann, M. I. Katsnelson, I. L. Soroka, O. Eriksson, and B. Hjörvarsson, Phys. Rev. B **69**, 064411 (2004).
[13] C. A. Ramos, E. Vassallo Brigneti, J. Gómez, and A. Butera, Physica B **404**, 2784 (2009).
[14] A. Hubert and R. Schäfer, *Magnetic Domains*, 3rd ed. (Springer, New York, 2009).
[15] A. L. Sukstanskii and K. I. Primak, J. Magn. Magn. Mater. **169**, 31 (1997).
[16] V. Gehanno, R. Hoffmann, Y. Samson, A. Marty, and S. Auffret, Eur. Phys. J. B **10**, 457 (1999).
[17] F. E. Spada, F. T. Parker, C. L. Platt, and J. K. Howard, J. Appl. Phys. **94**, 5123 (2003).
[18] R. A. McCurrie and P. Gaunt, Philos. Mag. **13**, 567 (1966).
[19] K. Barmak, J. Kim, D. C. Berry, W. N. Hanani, K. Wierman, E. B. Svedberg, and J. K. Howard, J. Appl. Phys. **97**, 024902 (2005).
[20] P. Rasmussen, X. Rui, and J. E. Shield, Appl. Phys. Lett. **86**, 191915 (2005).
[21] S. N. Hsiao, F. T. Huan, H. W. Chang, H. W. Huang, S. K. Chen, and H. Y. Lee, Appl. Phys. Lett. **94**, 232505 (2009).
[22] J. A. Aboaf, T. R. McGuire, S. R. Herd, and E. Klokholm, IEEE Trans. Magn. **20**, 1642 (1984).
[23] H. Shima, K. Oikawa, A. Fujita, K. Fukamichi, and K. Ishida, J. Magn. Magn. Mater. **272-276**, 2173 (2004).
[24] W. Wunderlich, K. Takahashi, D. Kubo, Y. Matsumara, and Y. Nishi, J. Alloys Compd. **475**, 339 (2009).
[25] Y. Murayama, J. Phys. Soc. Jpn. **21**, 2253 (1966).
[26] C. Kooy and V. Enz, Philips Res. Rep. **15**, 7 (1960).
[27] N. Saito, H. Fujiwara, and Y. Sugita, J. Phys. Soc. Jpn. **19**, 1116 (1964).
[28] H. Fujiwara, N. Saito, and Y. Sugita, Appl. Phys. Lett. **4**, 199 (1964).
[29] S. S. Lehrer, J. Appl. Phys. **34**, 1207 (1963).
[30] R. Carey, E. D. Isaac, and B. W. J. Thomas, J. Phys. D: Appl. Phys. **2**, 679 (1969).
[31] L. M. Alvarez-Prado, G. T. Pérez, R. Morales, F. H. Salas, and J. M. Alameda, Phys. Rev. B **56**, 3306 (1997).